

Supplemental Material for paper “Second-Order Approximation for Variance Reduction in Multiple Importance Sampling”

H. Lu^{†1}
 R. Pacanowski^{‡1}
 X. Granier^{§1}
 Inria - Univ. Bordeaux/LaBRI
 CNRS/LP2N

1. MANAO: Inria Bordeaux Sud-Ouest - LP2N (Univ. Bordeaux, IOGS, CNRS) - LaBRI (Univ. Bordeaux, CNRS)

1 Different derivations

1.1 From Equation 2 to Equation 3

To estimate the integral of a function $L = \int f(\omega) d\omega$ using random samples $\{\omega_{i=B|L, n=1..N_i}\}$ from two PDFs p_B (for BRDF-based strategy to generate N_B samples) and p_L (for light-based strategy to generate N_L samples), Veach [VG95] has introduced the MIS estimator

$$L_{N_L, N_B} = \sum_{i=B|L} \frac{1}{N_i} \sum_{n=1}^{N_i} w_i(\omega_{i,n}) \frac{f(\omega_{i,n})}{p_i(\omega_{i,n})} \quad (2)$$

where $w_i(\omega_{i,n})$ is a weighting function. For balance heuristic,

$$w_i(\omega_{i,n}) = \frac{N_i p_i(\omega_{i,n})}{N_B p_B(\omega_{i,n}) + N_L p_L(\omega_{i,n})}.$$

By denoting $N = N_B + N_L$ (N is the total number of samples) and $N_B = \alpha N$,

$$w_B(\omega_{B,n}) = \frac{\alpha p_B(\omega_{B,n})}{\alpha p_B(\omega_{B,n}) + (1-\alpha) p_L(\omega_{B,n})}.$$

and

$$w_L(\omega_{L,n}) = \frac{(1-\alpha) p_L(\omega_{L,n})}{\alpha p_B(\omega_{L,n}) + (1-\alpha) p_L(\omega_{L,n})}.$$

Introducing everything in Equation 2 leads to

$$L_{\alpha N, (1-\alpha)N} = \frac{1}{\alpha N} \sum_{n=1}^{\alpha N} \frac{\alpha f(\omega_{B,n})}{\alpha p_B(\omega_{B,n}) + (1-\alpha) p_L(\omega_{B,n})} + \frac{1}{(1-\alpha)N} \sum_{n=1}^{(1-\alpha)N} \frac{(1-\alpha) f(\omega_{L,n})}{\alpha p_B(\omega_{L,n}) + (1-\alpha) p_L(\omega_{L,n})}$$

or

$$L_{N,\alpha} = \frac{1}{N} \sum_{n=1}^{\alpha N} \frac{f(\omega_{B,n})}{\alpha p_B(\omega_{B,n}) + (1-\alpha) p_L(\omega_{B,n})} + \frac{1}{N} \sum_{n=1}^{(1-\alpha)N} \frac{f(\omega_{L,n})}{\alpha p_B(\omega_{L,n}) + (1-\alpha) p_L(\omega_{L,n})}.$$

A simple change of indices from $\{(B, n = 1.. \alpha N)\}$ and $\{(L, n = 1.. (1-\alpha)N)\}$ to $\{i = 1..N\}$ leads to the Defensive Importance Sampling (DIS) [Hes95] formula

$$L_{N,\alpha} = \frac{1}{N} \sum_{i=1}^N \frac{f(\omega_i)}{\alpha p_B(\omega_i) + (1-\alpha) p_L(\omega_i)}. \quad (3)$$

1.2 Computing and Approximating $E[L_{1,\alpha}^2]$

Starting from DIS formulation in Equation 3, we have

$$L_{1,\alpha} = \frac{f(\omega_1)}{\alpha p_B(\omega_1) + (1-\alpha) p_L(\omega_1)}.$$

Since in the case of DIS, the PDF corresponding to the sampling strategy is $p_\alpha(\omega) = \alpha p_B(\omega) + (1-\alpha) p_L(\omega)$, we get

$$E[L_{1,\alpha}^2] = \int \left(\frac{f(\omega)}{p_\alpha(\omega)} \right)^2 p_\alpha(\omega) d\omega.$$

It is equivalent to

$$E[L_{1,\alpha}^2] = \int \frac{f^2(\omega)}{p_\alpha(\omega)} d\omega.$$

In the following, for legibility reasons, we will omit ω .

Introducing $\bar{p} = (p_B + p_L)/2$ and $\Delta p = (p_B - p_L)/2$, we have

$$p_\alpha = \bar{p} + (2\alpha - 1) \Delta p.$$

The Taylor expansion of the D -differentiable rational $1/p_\alpha$

is given by

$$\frac{1}{p_\alpha} \approx \sum_{d=0}^D (-1)^d (2\alpha - 1)^d \frac{\Delta p^d}{\bar{p}^{d+1}}.$$

Therefore, we get the final D th order Taylor expansion

$$E[L_{1,\alpha}^2] \approx \sum_{d=0}^D (-1)^d (2\alpha - 1)^d \int \frac{f^2 \Delta p^d}{\bar{p}^{d+1}}.$$

1.3 Minimization of the 2nd order approximation

To minimize $E[L_{1,\alpha}^2]$, we have to compute α such as

$$\frac{d}{d\alpha} E[L_{1,\alpha}^2] = 0.$$

Using the second-order approximation

$$E[L_{1,\alpha}^2] \approx \sum_{d=0}^2 (-1)^d (2\alpha - 1)^d \int \frac{f^2 \Delta p^d}{\bar{p}^{d+1}},$$

leads to the linear form

$$\frac{d}{d\alpha} E[L_{1,\alpha}^2] \approx \sum_{d=1}^2 (-1)^d 2d (2\alpha - 1)^{d-1} \int \frac{f^2 \Delta p^d}{\bar{p}^{d+1}},$$

or more simply

$$\frac{d}{d\alpha} E[L_{1,\alpha}^2] \approx -2 \int \frac{f^2 \Delta p}{\bar{p}^2} + 4 (2\alpha - 1) \int \frac{f^2 \Delta p^2}{\bar{p}^3}.$$

This approximation is equal to zero when

$$2\alpha - 1 = \frac{1}{2} \left(\int \frac{f^2 \Delta p}{\bar{p}^2} / \int \frac{f^2 \Delta p^2}{\bar{p}^3} \right).$$

1.4 Theoretical Accuracy for Two Cases

Since it is based on an approximation, our approach has limited accuracy. We estimate it for two cases: perfect mirror BRDF where α has to be 1 and Dirac light source where α has to be 0.

For highly specular cases, BRDFs are zero in almost every direction excepted in a small direction domain. And the shading function follows the same behavior. In this domain, $p_B(\omega)$ is thus very large, therefore, Δp and \bar{p} might be approximated simply by p_B .

Consequently

$$2\alpha - 1 = \frac{1}{2} \left(\int \frac{f^2 p_B}{p_B^2} / \int \frac{f^2 p_B^2}{p_B^3} \right),$$

or

$$2\alpha - 1 = \frac{1}{2} \left(\int \frac{f^2}{p_B} / \int \frac{f^2}{p_B} \right),$$

Finally

$$2\alpha - 1 = \frac{1}{2} \Leftrightarrow \alpha = 3/4.$$

Reciprocally, the same demonstration for very concentrated light source leads to

$$2\alpha - 1 = -\frac{1}{2} \Leftrightarrow \alpha = 1/4.$$

1.5 Theoretical Variance Reduction

In this section, we denote $p_\alpha = \alpha p_L + (1 - \alpha) p_B$ and $p_{1/2} = (p_L + p_B)/2$. With such a notation the difference of variance Δ_N is expressed as

$$\Delta_N = V[L_{N,\alpha}] - V[L_{N,1/2}] = \frac{1}{N} \Delta_1$$

with $\Delta_1 = V[L_{1,\alpha}] - V[L_{1,1/2}]$. In the following, we will focus on variance reduction expressed by Δ_1 . We have

$$\Delta_1 = E[L_{1,\alpha}^2] - E[L_{1,\alpha}]^2 - E[L_{1,1/2}^2] + E[L_{1,1/2}]^2.$$

Since we assume unbiased sampling for all α , we have $E[L_{1,\alpha}] = E[L_{1,1/2}] = L$. Δ_1 is thus simplified to

$$\Delta_1 = E[L_{1,\alpha}^2] - E[L_{1,1/2}^2] = \int \left(\frac{f}{p_\alpha} \right)^2 p_\alpha - \int \left(\frac{f}{p_{1/2}} \right)^2 p_{1/2}.$$

Factorization leads to

$$\begin{aligned} \Delta_1 &= \int \left(\frac{f}{p_\alpha} \right)^2 p_\alpha \left(1 - \frac{p_\alpha}{p_{1/2}} \right) \\ &= \int \left(\frac{f}{p_\alpha} \right)^2 p_\alpha \left(\frac{p_{1/2} - p_\alpha}{p_{1/2}} \right) \\ &= \int \left(\frac{f}{p_\alpha} \right)^2 p_\alpha (1/2 - \alpha) \left(\frac{p_B - p_L}{(p_B + p_L)/2} \right) \\ &= \int \left(\frac{f}{p_\alpha} \right)^2 p_\alpha (1 - 2\alpha) \left(\frac{p_B - p_L}{p_B + p_L} \right) \\ \Delta_1 &= (1 - 2\alpha) \int \left(\frac{f}{p_\alpha} \right)^2 p_\alpha \left(\frac{p_B - p_L}{p_B + p_L} \right) \end{aligned}$$

By taking the absolute value

$$|\Delta_1| = \beta_\alpha |2\alpha - 1|$$

where $\beta_\alpha = \left| \int \left(\frac{f}{p_\alpha} \right)^2 p_\alpha \left(\frac{p_B - p_L}{p_B + p_L} \right) \right|$. Unfortunately, it is difficult to have an exact solution. However, we can provide a theoretical and conservative upper bound. For this purpose, we notice that

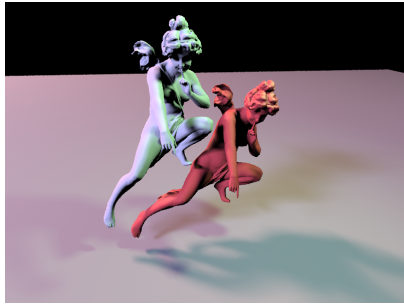
$$\beta_\alpha \leq \int \left(\frac{f}{p_\alpha} \right)^2 p_\alpha \left| \frac{p_B - p_L}{p_B + p_L} \right|.$$

Since $p_B \geq 0$ and $p_L \geq 0$,

$$\left| \frac{p_B - p_L}{p_B + p_L} \right| \leq 1$$

Therefore

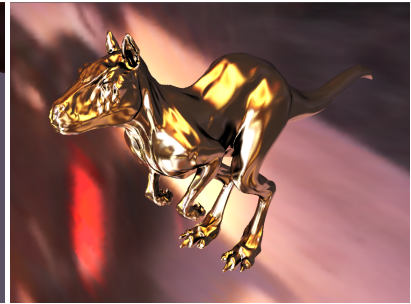
$$\beta_\alpha \leq \int \left(\frac{f}{p_\alpha} \right)^2 p_\alpha = E[L_{1,\alpha}^2] = V[L_{1,\alpha}] + L^2.$$



Scene 3
Diffuse BRDFs
Three area light sources



Scene 4
Diffuse BRDFs
High-frequency environment map



Scene 5
Highly specular BRDF
High-frequency environment map
+ 1 point light source



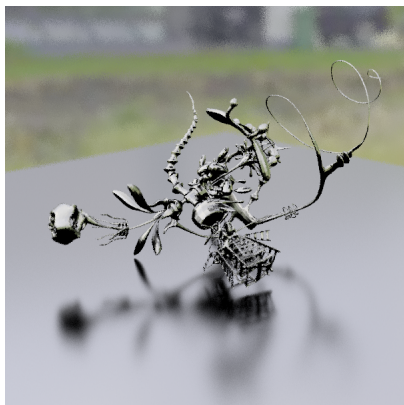
Scene 6
Diffuse BRDFs
Area light source
+ 1 point light source



Scene 7
Glossy BRDF
Low-frequency environment map



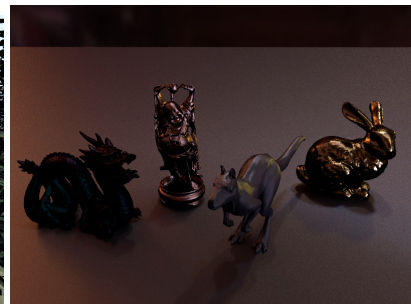
Scene 8
Mirror BRDF
High-frequency environment map



Scene 9
Glossy BRDFs and complex visibility
Low-frequency environment map



Scene 10
Diffuse BRDFs and complex visibility
Low-frequency environment map
+ 1 point and 1 directional light sources



Scene 11
Measured glossy BRDFs
High-frequency environment map

Figure 1: Our test scenes, ranging from diffuse (scenes 3, 4 and 6) to specular (scenes 8 and 2) materials including complex visibility (scene 10) with different types of illumination such as area light sources (scenes 1, 3 and 6) and environment maps. Since only one sample is required for point and directional light sources, their contribution are added separately and we exclude them from variance computation.

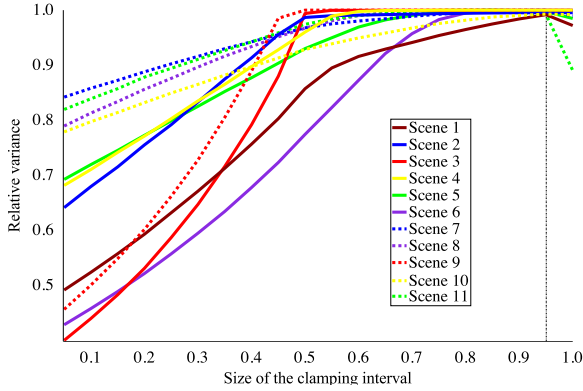


Figure 2: Effect of clamping α for each scene. The y-axis represents the variance for $L_{N,\alpha}$, relatively to the best variance (cf. Figure 7). The x-axis represents the size of an interval centered at $1/2$ that restricts the value of α . When the size of the validity domain is equal to zero, this corresponds to the default balance heuristic. For each scene, the number of samples per light source to estimate α is set to $M = 128$ and the one to compute the variance to $N = 256$.

Because, we expect variance improvement with the optimization method, we have $V[L_{1,\alpha}] \leq V[L_{1,1/2}]$ with this assumption,

$$\left| V[L_{1,\alpha}] - V[L_{1,1/2}] \right| \leq |2\alpha - 1| \left(V[L_{1,1/2}] + L^2 \right).$$

2 Clamping interval for α

Figure 2 shows the effect of clamping α for each test scene. As explained in the paper, this experiment confirms two facts. First, the second-order approximation is not sufficient to capture some variance oscillations in the interval $[0, 1]$ since clamping improves the results. Second, it also confirms that our estimation still provide a good hint of what is the dominant strategy. It also justifies our clamping of α to $[0.025, 0.975]$ for all our results.

3 More Variance Analysis

As illustrated in Figure 3, for a fixed number of samples M for α estimation, increasing the number of samples N for shading will make more and more samples benefit from our method. Therefore, the sampling variance $V[L_{1,\alpha}]$ also decreases. Note that, because of the low number of samples M , the quality of α cannot be always as good as the preprocessed one, which is computed with $M = 4096$. However, a low-quality α value still helps reducing the sampling variance. As shown in Figure 4, with the same conditions of Figure 3, the variance of $L_{N,\alpha}$ also benefits from the sampling variance. For a given value of α , $V[L_{1,\alpha}]$ is fixed and our method converges faster than the default balance heuristic. This illustrated by the fact that the lines of our method are all below the black one which represents the balance heuristic.

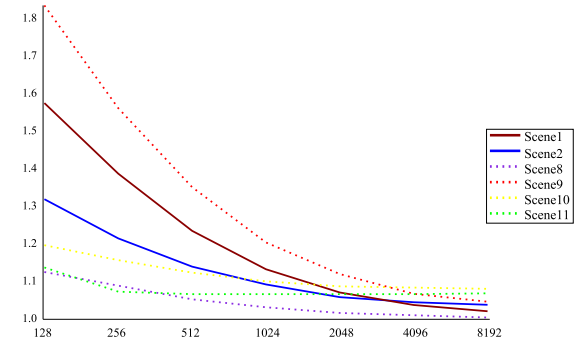


Figure 3: Plot of the relative variance for $V[L_{1,\alpha}]$ (y-axis), with a fixed number of samples $M = 128$ to estimate α for different number of samples N (x-axis). The y-axis represents the variance divided by the variance obtained when computing α with $M = 4096$. When the number of samples N increases, more samples benefit from our integrated estimation (cf. Equation 6 in the paper) and therefore the variance of $L_{1,\alpha}$ is also reduced.

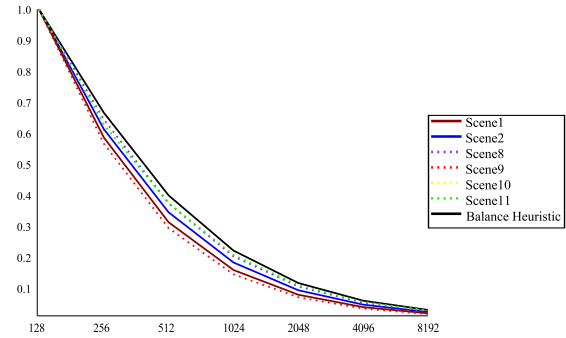


Figure 4: Plot of the relative variance for $V[L_{N,\alpha}]$ (y-axis), with a fixed number of samples $M = 128$ to estimate α for different number of samples N (x-axis). The y-axis represents the relative variance for $L_{N,\alpha}$: $V(L_{N,\alpha})/V(L_{N=128,\alpha})$. Our method converges faster than default balance heuristic when increasing number of samples N for shading.

4 Equal Time Comparisons

In order to visualize the efficiency of our method, we report equal time comparisons for different test scenes (cf. Figures 5 and 6). These results are generated by adjusting the number of samples per light source for the balance heuristic in order to match the rendering time of our method when using $N = 256$ samples per light source (cf. Equation 7 in the paper with $M = 128$). Our α estimation changes the weights of using different sampling strategies allowing to more samples for the same rendering time (Scenes 8 and 11). Although, our method requires less samples for Scenes 1, 2 and 9, our method still gives better results. Especially in shadows and highlights where we have less noise. The estimator variance $V[L_{N,\alpha}]$ is reported here, rather than the sampling

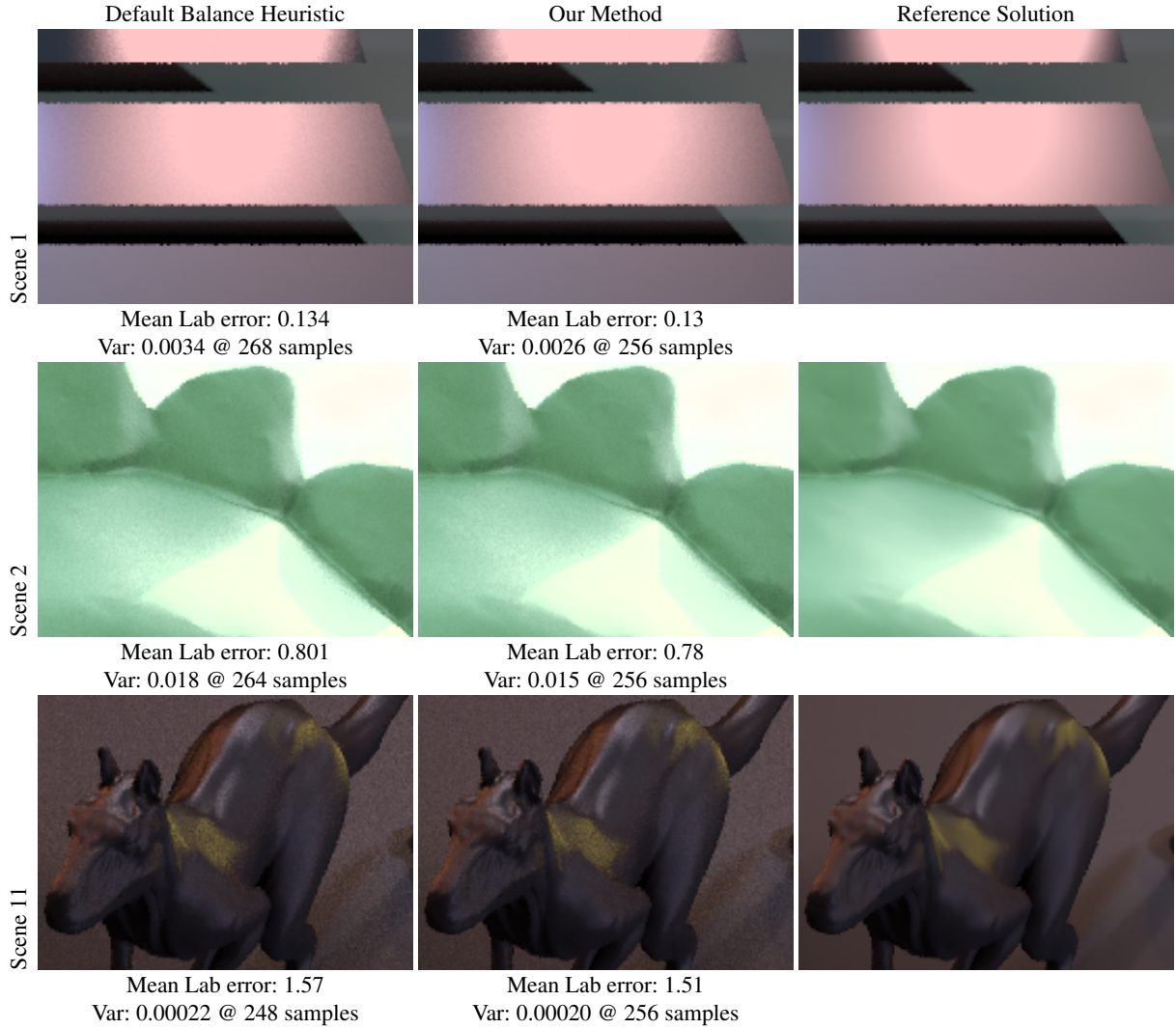


Figure 5: Close-up views for *Scenes 1, 2 and 11*. Equal time comparisons between (*Left*) balance heuristic and (*Center*) our method against (*Right*) a reference solution computed with 32768 samples per light source. For each scene we report the mean Lab error, the estimator variance $V[L_{N,\alpha}]$ and the number of samples per light source for the full image shown in Figure 1.

variance $V[L_{1,\alpha}]$, since the latter one is not impacted by the number of samples N .

5 Other results

5.1 Per-pixel α values

Per-pixel α values (cf. Figures 8 and 9) are presented as RGB colors, the RGB color for each pixel is computed as:

$$(R, G, B) = \left(\frac{\alpha}{\max(\alpha, 1-\alpha)}, \frac{1-\alpha}{\max(\alpha, 1-\alpha)}, 0 \right)$$

where the perfect red means samples are all selected from light sources, the perfect green means from BRDFs, and the perfect yellow means the classical half-half strategy.

5.1.1 Per-pixel α values for Each Light Source

The α value is computed for each light source and can thus be also visualized separately. We illustrate this feature in Figure 9 on scene 1. It clearly shows that the larger the light source is and the closer it is to a glossy BRDF, the more samples from BRDF will be used.

5.2 Lab Difference Images

Figure 10 and Figure 11 present, for each scene, Lab difference images between our balancing method and their corresponding reference solution. Each Lab image is computed from an LDR image obtained after applying the tone-

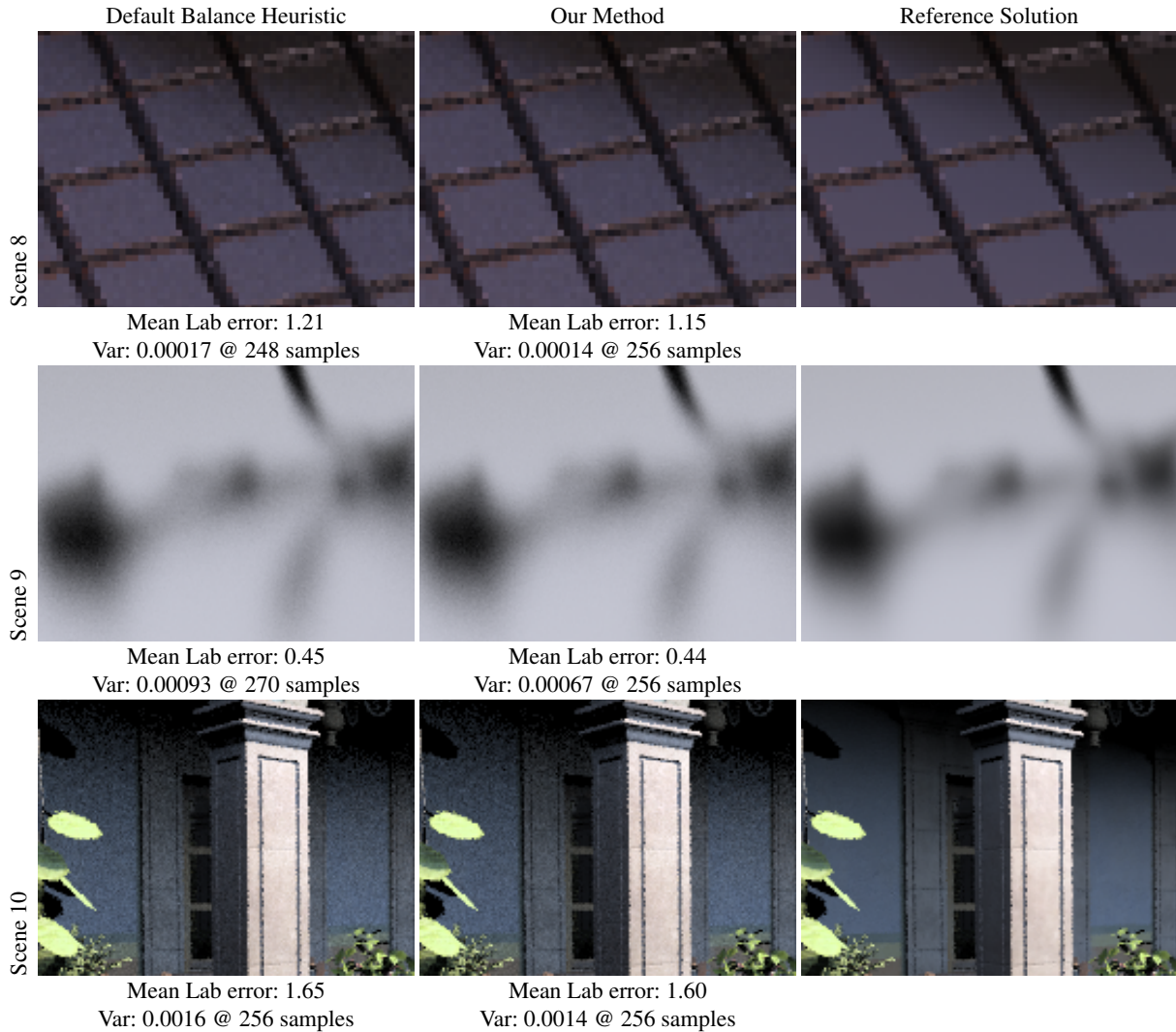


Figure 6: Close-up views for *Scenes 8 to 10*. Equal time comparisons between (**Left**) balance heuristic and (**Center**) our method against (**Right**) a reference solution computed with 32768 samples per light source. For each scene we report the mean Lab error, the estimator variance $V[L_{N,\alpha}]$ and the number of samples per light source for the full image shown in Figure 1.

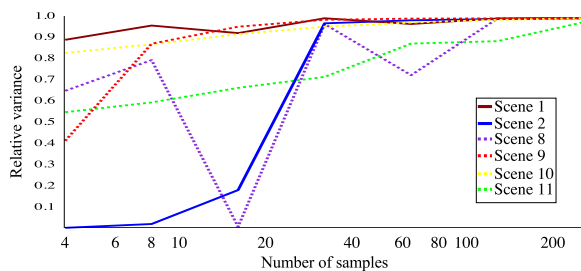


Figure 7: Number of samples M to estimate α per scene. The y-axis represents the variance for $L_{N,\alpha}$ ($N = 256$), relatively to the best variance obtained by our technique with different value of M for a given scene, thus illustrates the convergence of α estimation.

mapping operator (gamma correction) to the corresponding original HDR image.

References

- [Hes95] HESTERBERG T.: Weighted Average Importance Sampling and Defensive Mixture Distributions. *Technometrics* 37, 2 (1995), 185–194. 1
- [Vea98] VEACH E.: *Robust monte carlo methods for light transport simulation*. PhD thesis, 1998. Stanford University. 7
- [VG95] VEACH E., GUIBAS L. J.: Optimally combining sampling techniques for Monte Carlo rendering. In *Proc. ACM SIGGRAPH'95* (1995), ACM, pp. 419–428. 1

Method	Scene										
	1	2	3	4	5	6	7	8	9	10	11
BRDF	67.3	4597	24.14	0.294	0.469	1.260	5.39	2.070	0.0198	139.75	0.378
Light	0.47	2.56	0.005	0.014	4.131	0.088	61.7	0.036	118.20	0.776	0.127
Balanced heuristic	0.90	4.76	0.096	0.027	0.410	0.120	5.76	0.043	0.250	0.402	0.055
Power heuristic	0.99	4.87	0.097	0.030	0.450	0.138	6.42	0.046	0.255	0.440	0.059
Maximum heuristic	1.24	5.11	0.097	0.035	0.550	0.157	9.78	0.061	0.256	0.618	0.075
Preprocessed α	0.42	2.95	0.035	0.016	0.27	0.047	5.09	0.033	0.095	0.301	0.045

Table 1: Comparisons, for each scene, of different balancing methods in terms of average sampling variance. The average variances are computed over all the pixels using the same number of samples $N = 256$ for each light source.

	Method	Scene										
		1	2	3	4	5	6	7	8	9	10	11
Var.	cf. Table 1											
	Integrated estimation of α	0.66	3.88	0.065	0.022	0.35	0.086	5.68	0.037	0.1700	0.359	0.051
Lab error	BRDF	14.9	6.5	10.5	2.80	1.10	22.9	2.00	3.85	0.36	5.26	3.38
	Light	0.14	1.11	0.25	0.78	7.50	0.23	3.60	1.16	15.9	2.00	2.25
	Balance heuristic	0.14	0.81	0.31	0.91	0.77	0.28	1.04	1.21	0.47	1.65	1.54
	Power heuristic	0.11	0.83	0.31	0.93	0.78	0.28	1.06	1.22	0.46	1.70	1.59
	Maximum heuristic	0.12	0.95	0.31	0.99	0.85	0.28	1.30	1.37	0.45	1.98	1.71
	Integrated estimation of α	0.13	0.78	0.29	0.86	0.74	0.26	1.02	1.15	0.44	1.60	1.51
Time (sec.)	BRDF	158.6	138.1	40.6	55.1	33.7	16.9	59.1	36.5	49.2	354	91.0
	Light	299.7	102.8	147.4	41.8	18.6	33.8	41.7	34.2	27.1	178	53.0
	Balance heuristic	237.7	123.5	95.5	48.9	28.0	25.5	52.0	36.2	40.0	281	74.0
	Power heuristic	239.9	122.3	95.7	48.8	27.1	24.9	49.9	35.9	39.2	275	74.0
	Maximum heuristic	239.0	121.6	95.4	48.1	26.0	24.5	49.5	34.9	38.5	264	71.1
	Integrated estimation of α	250.8	128.3	106.9	45.8	28.3	26.9	51.1	34.5	40.9	281	72.0
Efficiency	BRDF	0.0001	0.0000	0.0010	0.0617	0.0633	0.0470	0.0031	0.0132	1.0265	0.0000	0.0291
	Light	0.0071	0.0038	1.3569	1.7088	0.0130	0.3362	0.0004	0.8122	0.0003	0.0072	0.1486
	Balance heuristic	0.0047	0.0017	0.1091	0.7574	0.0871	0.3268	0.0033	0.6424	0.1000	0.0089	0.2457
	Power heuristic	0.0042	0.0017	0.1077	0.6831	0.0820	0.2910	0.0031	0.6055	0.1000	0.0083	0.2290
	Maximum heuristic	0.0034	0.0016	0.1081	0.5940	0.0699	0.2600	0.0021	0.4697	0.1015	0.0061	0.1875
	Integrated estimation of α	0.0060	0.0020	0.1439	0.9925	0.1010	0.4323	0.0034	0.7834	0.1438	0.0099	0.2723

Table 2: Average variance and Lab error, rendering time and efficiency for each scene and for different balancing methods. We use $N = 256$ samples per light source for each method. Integrated estimation of α refers to the estimator introduced in Equation 7 in the paper where we use half of the total samples to evaluate α ($M = 128$) and the remaining half to evaluate the radiance with the estimated α . The Lab error is computed against the reference solution. The efficiency [Vea98] of each strategy is computed as the inverse of the product of the variance and the rendering time.

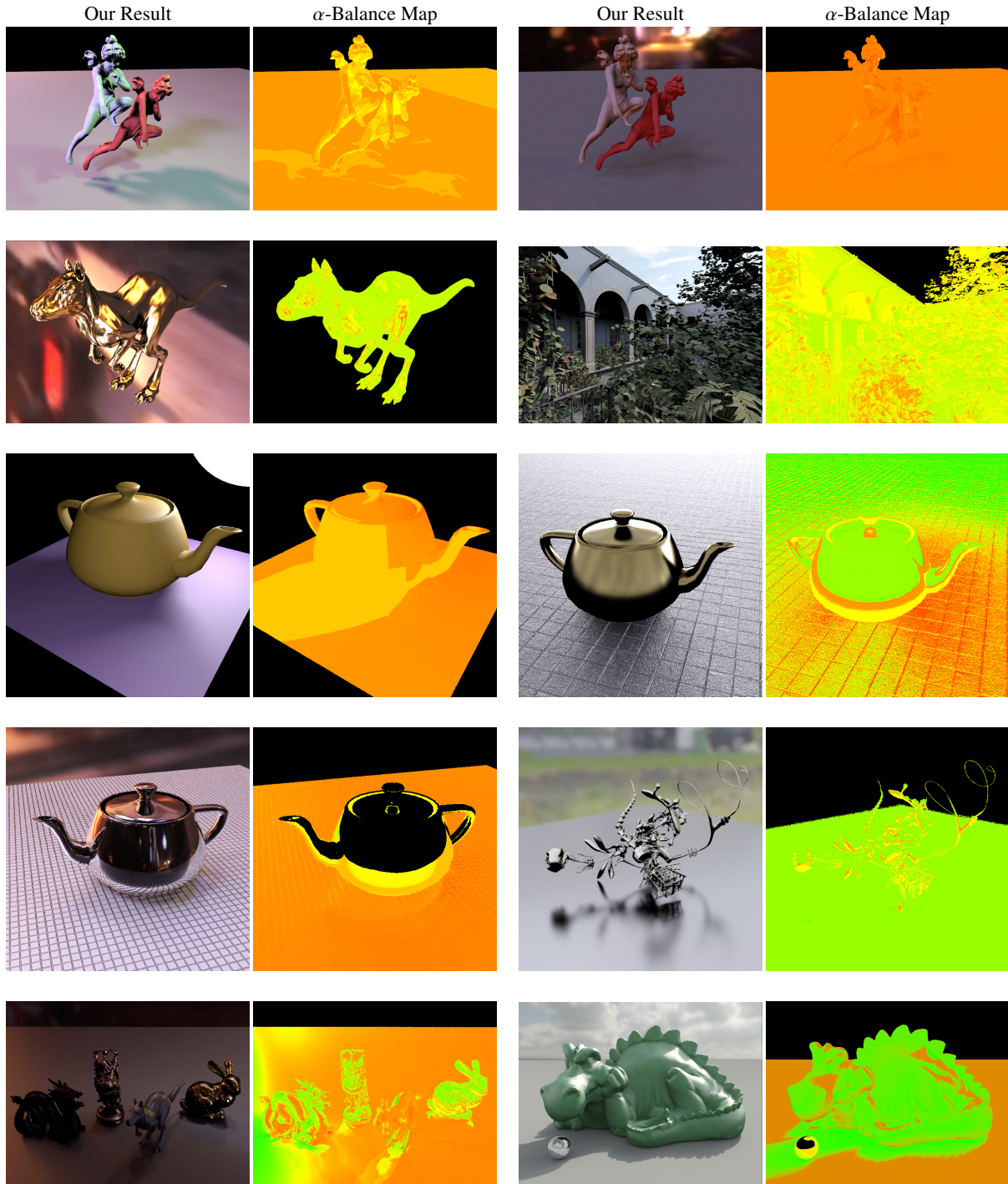


Figure 8: Per-pixel α values. For each scene we show (**Left**) our result and (**Right**) the α -balance map, which represents how the α value varies spatially.

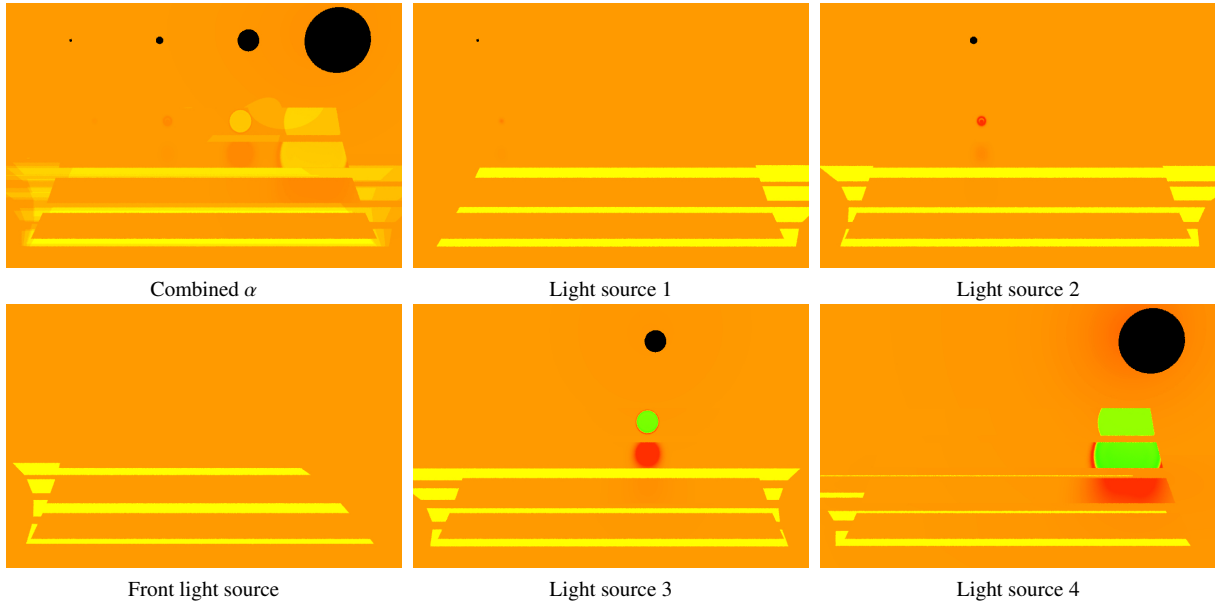


Figure 9: (Scene 1). Per-pixel α value for each of the five light sources. One light source is not directly visible since it is facing the whole scene.

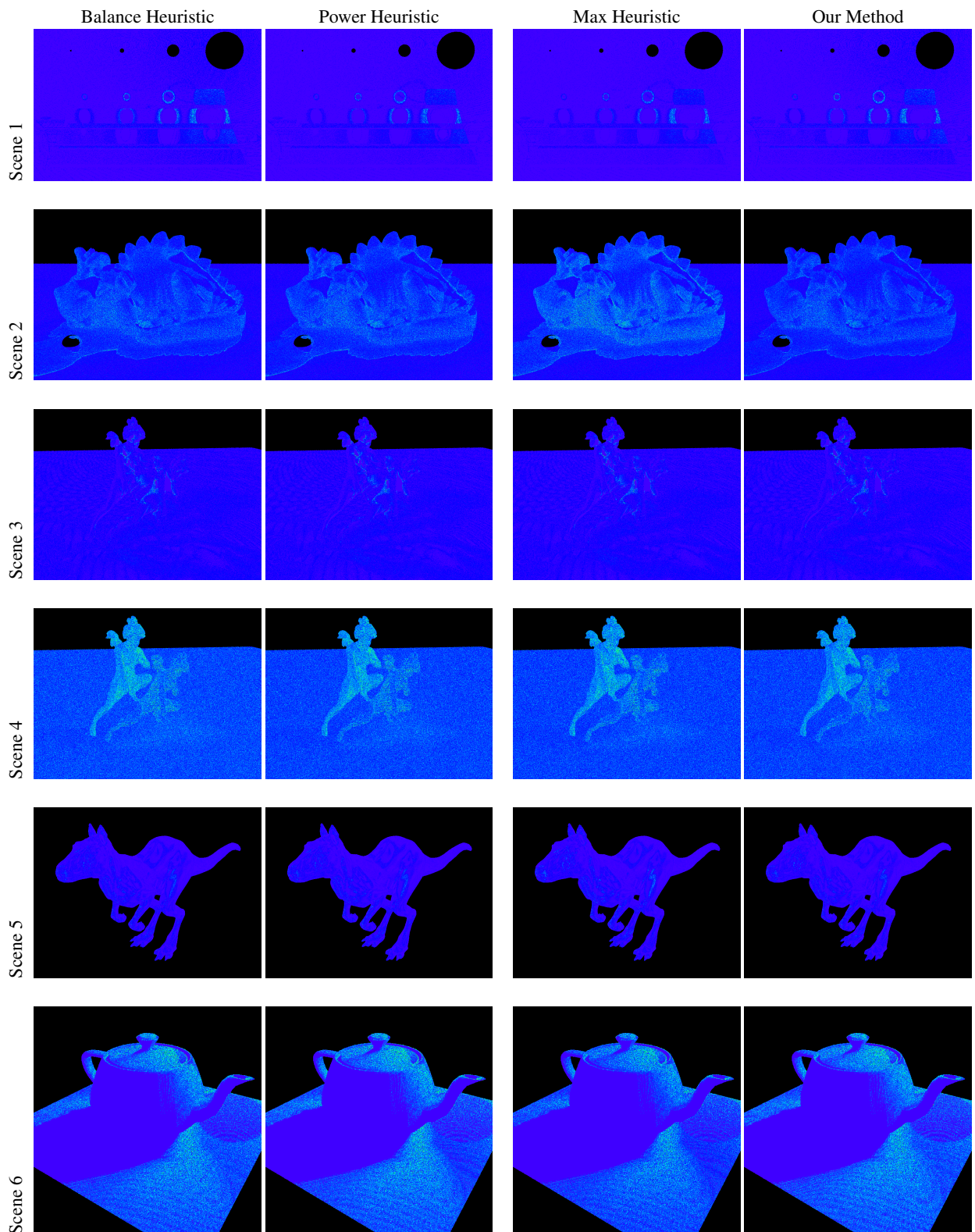


Figure 10: Lab difference images computed against a reference solution rendered with 32768 samples per light source.

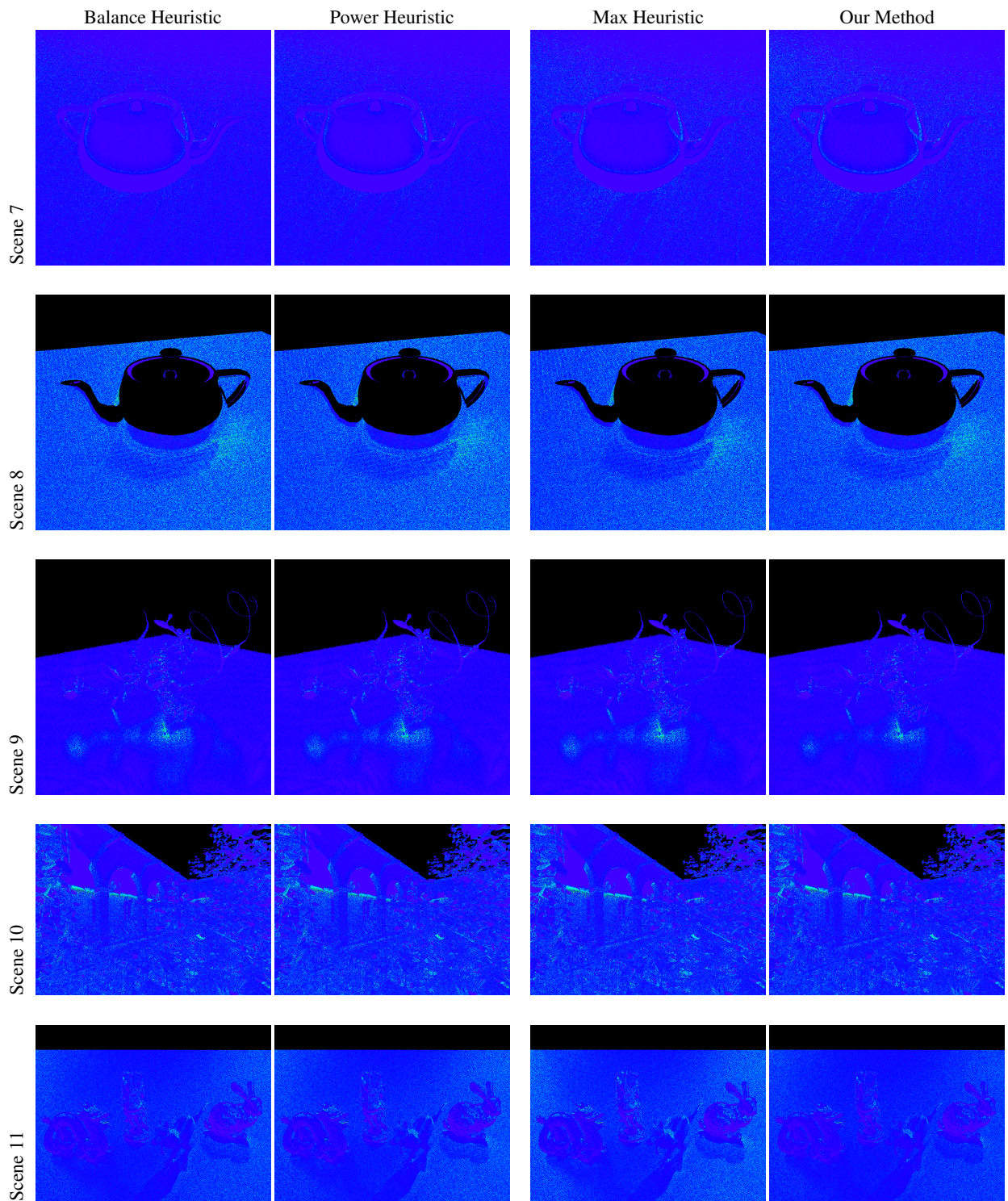


Figure 11: Lab difference images computed against a reference solution rendered with 32768 samples per light source.